

Nonlocal Pseudopotential Energy Density Functional for Orbital-Free Density Functional Theory

Qiang Xu,¹ Cheng Ma,¹ Wenhui Mi,¹ Yanchao Wang,^{1,*} and Yanming Ma^{1,2,†}

*¹International Center for Computational Methods and
Software & State Key Lab of Superhard Materials,
College of Physics, Jilin University, Changchun 130012, China.*

*² International Center of Future Science,
Jilin University, Changchun 130012, China.*

Abstract

Orbital-free density functional theory (OF-DFT) runs at low computational cost that scales linearly with the number of simulated atoms, making it suitable for large-scale material simulations. It is generally considered that OF-DFT strictly requires the use of local pseudopotentials, rather than orbital-dependent nonlocal pseudopotentials, for the calculation of electron-ion interaction energies, as no orbitals are available. This is unfortunate situation since the nonlocal pseudopotentials are known to give much better transferability and calculation accuracy than local ones. We report here the development of a theoretical scheme that allows the direct use of nonlocal pseudopotentials in OF-DFT. In this scheme, a nonlocal pseudopotential energy density functional is derived by the projection of nonlocal pseudopotential onto the non-interacting density matrix (instead of “orbitals”) that can be approximated explicitly as a functional of electron density. Our development defies the belief that nonlocal pseudopotentials are not applicable to OF-DFT, leading to the creation of an alternate theoretical framework of OF-DFT that works superior to the traditional one.

Ab initio calculations using Kohn-Sham (KS) density functional theory (DFT)[1, 2] can accurately describe the fundamental properties of various materials. However, its computational cost scales with the cube of the number of electrons in the simulation cell, which poses a major challenge to large-scale simulations. In contrast, orbital-free (OF) DFT runs with a much lower computational cost that scales linearly with the number of atoms in the system, as it relies only on electron density and the use of KS orbitals is avoided. As a result, OF-DFT is successfully applied to large-scale simulations of systems with up to millions of atoms[3–6].

The accuracy of OF-DFT simulations depends strongly on the evaluation of the non-interacting kinetic energy and the electron–ion (or electron–pseudocore) interaction energy. Many approximate kinetic energy density functionals (KEDFs) have been proposed to evaluate the non-interacting kinetic energy in OF-DFT[7–39]. Their use in combination with local pseudopotentials[40–44] can achieve results that agree reasonably with those derived by KS-DFT, especially for main-group metals, III–V semiconductors[24, 34, 36, 45], and even systems with inhomogeneous electron density such as metal clusters and quantum dots[37, 39].

Unfortunately, the local pseudopotentials [28, 31, 32, 40, 41, 43] used to evaluate the electron–ion interaction energy suffer from a lack of transferability[43], as they fail to reproduce the correct scattering behavior of the all-electron potentials[46–48]. Overcoming the transferability problem requires a reliance on all-electron potential or nonlocal pseudopotentials (NLPPs), which are widely used in orbital-based approaches. However, it is practically infeasible to use the all-electron potential, as an accurate all-electron KEDF for OF-DFT calculations is missing[49, 50]. Furthermore, the use of NLPPs[46, 51] runs against conventional understanding, as no orbitals are available in the traditional framework of OF-DFT[41, 42, 44, 52, 53].

A crucial nonlocal energy term with a set of angular-momentum-dependent energies has recently been added to OF-DFT calculations[54, 55] in an effort to correct errors arising from the use of KEDFs and local pseudopotentials. This approach has successfully reproduced the bulk properties of several standard structures of Ti. However, special care must be taken when applying it to a wide range of practical simulations, as frozen on-site orbitals and empirically directed fitting parameters inevitably exist[52]. There is substantial demand for a general approach to evaluate the electron–ion interaction energy using NLPPs in OF-DFT

calculations. In this letter, we developed a theoretical scheme that allows the direct use of the NLPPs for the calculation of electron-ion interaction energy in OF-DFT, together with a specially designed theoretical framework of OF-DFT not known thus. This development leads to a OF-DFT calculation that gives a better transferability than before ever known.

In general, the total energy density functional of OF-DFT can be expressed as:

$$E[\rho] = T_s[\rho] + E_H[\rho] + E_{XC}[\rho] + \int V_{loc}(\mathbf{r})\rho(\mathbf{r})d^3\mathbf{r} + E_{II}(\{R_a\}), \quad (1)$$

where ρ , T_s , E_H , E_{XC} , V_{loc} , E_{II} , and $\{R_a\}$ are the electron density, KEDF, Hartree energy, exchange-correlation energy, local pseudopotential, ion-ion repulsion energy, and the set of atomic positions, respectively. To include the nonlocal electron-ion interactions, the total energy density functional of OF-DFT is reformulated as:

$$E[\rho] = T_s[\rho] + E_H[\rho] + E_{XC}[\rho] + \underbrace{\int V_{loc}(\mathbf{r})\rho(\mathbf{r})d^3\mathbf{r} + E_{nl}[\rho]}_{E_{EI}[\rho]} + E_{II}(\{R_\alpha\}), \quad (2)$$

where the total electron-ion interaction energy $E_{EI}[\rho]$ can be separated in two parts: a local part $E_{loc}[\rho] = \int \rho(\mathbf{r})V_{loc}(\mathbf{r})d^3\mathbf{r}$ and a nonlocal part $E_{nl}[\rho]$. All of the terms in Eq. (2) except the nonlocal part of pseudopotential ($E_{nl}[\rho]$), can be evaluated easily.

The exact nonlocal pseudopotential energy depends on the KS orbitals or the density matrix:

$$\begin{aligned} E_{nl} &\equiv \sum_i f_i \int \int \psi_i^*(\mathbf{r}')V_{nl}(\mathbf{r}', \mathbf{r})\psi_i(\mathbf{r})d^3\mathbf{r}d^3\mathbf{r}' \\ &= \int \int V_{nl}(\mathbf{r}', \mathbf{r})\gamma_s(\mathbf{r}, \mathbf{r}')d^3\mathbf{r}d^3\mathbf{r}', \end{aligned} \quad (3)$$

where f_i , $V_{nl}(\mathbf{r}', \mathbf{r}) = \langle \mathbf{r}' | \hat{V}_{nl} | \mathbf{r} \rangle$, and $\gamma_s(\mathbf{r}, \mathbf{r}') = \sum_i f_i \psi_i(\mathbf{r})\psi_i^*(\mathbf{r}')$ represent the occupation number of the i -th KS orbital ψ_i , the real-space representation of the nonlocal part pseudopotential, and the noninteracting density matrix, respectively. Considering that the density matrices $\gamma_s[\rho](\mathbf{r}, \mathbf{r}')$ can be used to approximate the KEDFs[7, 56, 57], a nonlocal pseudopotential energy density functional (NLPPF) relying directly on the density matrices was proposed to evaluate the nonlocal electron-ion interaction energy. The nonlocal electron-ion interaction energy is then rewritten as

$$E_{nl}[\rho] = \int \int V_{nl}(\mathbf{r}', \mathbf{r})\gamma_s[\rho](\mathbf{r}, \mathbf{r}')d^3\mathbf{r}d^3\mathbf{r}'. \quad (4)$$

By taking the Kleinman-Bylander form[58] of norm-conserving NLPPs, the nonlocal part [59] can be written as

$$V_{nl}(\mathbf{r}', \mathbf{r}) = \sum_{a,lm} E_{KB}^{a,lm} \chi_{lm}^a(\mathbf{r}') \chi_{lm}^{a*}(\mathbf{r}), \quad (5)$$

where $E_{KB}^{a,lm} = [\int \phi_{lm}^{a*}(\mathbf{r}) \delta V_l^a(\mathbf{r}) \phi_{lm}^a(\mathbf{r}) d^3\mathbf{r}]^{-1}$ and $\chi_{lm}^a(\mathbf{r}) = \delta V_l^a(\mathbf{r}) \phi_{lm}^a(\mathbf{r})$. The terms ϕ_{lm}^a and δV_l^a are the atomic pseudo-wave-function and the short-range pseudopotential corresponding to the lm -th angular momentum of a -th atom, respectively. $\gamma_s[\rho]$ denotes the density matrix as a functional of electron distribution ρ . Although there is no exact analytic form available for the density matrix functional, a modified Gaussian (MG)[60] form derived from the second-order Taylor expansions of the density matrix[61] was employed to approximate the density matrix functional:

$$\gamma_s^{MG}[\rho](\mathbf{r}, \mathbf{r}') = \rho(\bar{\mathbf{r}}) e^{-\frac{s^2}{2\beta(\bar{\mathbf{r}})}} \left[1 + A \left(\frac{s^2}{2\beta(\bar{\mathbf{r}})} \right)^2 \right], \quad (6)$$

where $s = |\mathbf{r} - \mathbf{r}'|$ and $\bar{\mathbf{r}} = (\mathbf{r} + \mathbf{r}')/2$. The parameter A is taken in the MG density matrix functional to achieve the $O(s^4)$ correction[60]. $\beta(\mathbf{r})$ denotes the ‘‘local temperature’’ $\beta(\mathbf{r}) = \frac{3}{2} \frac{\rho(\mathbf{r})}{t_s(\mathbf{r})}$ [62, 63], where $t_s(\mathbf{r})$ is the exact kinetic energy density defined as $t_s(\mathbf{r}) = t_s^{KS}(\mathbf{r}) \equiv \sum_{i=1}^{Occ.} \frac{1}{8} |\nabla \rho_i(\mathbf{r})|^2 / \rho_i(\mathbf{r}) - \frac{1}{8} \nabla^2 \rho(\mathbf{r})$ and $\rho_i(\mathbf{r}) = |\psi_i(\mathbf{r})|^2$ is i -th KS orbital’s density (see Refs.[60, 61]). To remove the orbital-dependent problem in $t_s(\mathbf{r})$ and obtain a solely density-dependent form of the density matrix functional, the kinetic energy density is obtained directly from the integrand of KEDFs to replace the exact one: $t_s(\mathbf{r}) \approx t_s[\rho](\mathbf{r})$. The widely used Wang-Teter (WT) KEDF[28] is chosen as an exemplary case, and $t[\rho](\mathbf{r})$ can be expressed as

$$t_s^{WT}[\rho](\mathbf{r}) = \frac{3}{10} (3\pi^2)^{2/3} \rho^{5/3}(\mathbf{r}) + \frac{1}{8} \frac{|\nabla \rho(\mathbf{r})|^2}{\rho(\mathbf{r})} + \rho^{5/6}(\mathbf{r}) \int \omega_{WT}(\mathbf{r}, \mathbf{r}') \rho^{5/6}(\mathbf{r}') d^3\mathbf{r}', \quad (7)$$

where $\omega_{WT}(\mathbf{r}, \mathbf{r}')$ is the kernel of WT functional. The Supplemental Material[64] gives details of the kinetic energy density obtained from the WT KEDF.

The direct numerical evaluations of $\rho(\bar{\mathbf{r}})$ and $\beta(\bar{\mathbf{r}})$ at the average position $\bar{\mathbf{r}}$ are very complicated. They are therefore approximated using q -mean ‘‘nonlocal density’’ $\rho_q(\mathbf{r}, \mathbf{r}') = \left[\frac{\rho^q(\mathbf{r}) + \rho^q(\mathbf{r}')}{2} \right]^{1/q}$ and two-point average temperature $\beta(\mathbf{r}, \mathbf{r}') = [\beta(\mathbf{r}) + \beta(\mathbf{r}')]/2$ for systems with slowly varying electron densities. The density matrix functional of Eq. (6) can then be reformulated as

$$\tilde{\gamma}_s^{MG}[\rho](\mathbf{r}, \mathbf{r}') = \rho_q(\mathbf{r}, \mathbf{r}') e^{-\frac{s^2}{2\beta(\mathbf{r}, \mathbf{r}')}} \left[1 + A \left(\frac{s^2}{2\beta(\mathbf{r}, \mathbf{r}')} \right)^2 \right]. \quad (8)$$

Combining Eqs. (4), (5) and (8) gives the NLPPF as

$$E_{nl}[\rho] \approx \sum_{a,lm} E_{KB}^{a,lm} \int_{\Omega_a} \int_{\Omega_a} \chi_{lm}^a(\mathbf{r}') \chi_{lm}^{a*}(\mathbf{r}) \tilde{\gamma}_s^{MG}[\rho](\mathbf{r}, \mathbf{r}') d^3\mathbf{r} d^3\mathbf{r}', \quad (9)$$

where the integral domain Ω_a is the a -th ionic core region. Owing to the short-range nature of $\{\chi_{lm}^a(\mathbf{r})\}$, the computational cost of Eq. (9) scales linearly $\mathcal{O}[cN_a]$ with the number of atoms (N_a), where c can be regarded as a constant derived from the double integral within the near-core region. Within the NLPPF scheme, a new theoretical framework of OF-DFT has been built and implemented in ATLAS[5, 65]. The Supplemental Material [64] gives further computational details, including the generation of pseudopotentials [see TABLE SI] and the parameters (A, q) used in NLPPF [see TABLE SII].

We applied this framework for OF-DFT to calculations of Li, Mg, and Cs in a wide variety of crystal structures. For each structure, 13 energy–volume points were calculated by expanding and compressing the approximate equilibrium volume by up to 20%, and the bulk properties (the equilibrium cell volume V_0 , bulk modulus B_0 , and the relative energy E_R with respect to hexagonal-close-packed, HCP, structure) were determined by fitting the energy–volume curve against Murnaghan’s equation of state[66]. The comparison of the results obtained by OF-DFT using both local pseudopotentials (goLPS[44], BLPS[41], and OEPP[43]) and NLPPs against those calculated by KS-DFT using the projector augmented-wave (PAW)[67] method are presented in TABLE SIII of the Supplemental Material. For Li and Mg solids, the OF-DFT calculations within both local pseudopotentials and NLPPs give reasonable predictions of V_0 , B_0 , and E_R , which are comparable with the KS-DFT results. It is noteworthy that our scheme shows an improvement over the local pseudopotentials of OEPP for bulk Cs. The accurate bulk properties of Li, Mg, and Cs obtained by the current scheme demonstrate its valid applicability to simple metallic solids.

Further assessment of the accuracy of our scheme was by molecular dynamics calculations for Li-Mg alloy. The calculations used a canonical ensemble (at 1000K) in a supercell containing 108 atoms ($\text{Li}_{54}\text{Mg}_{54}$). The calculated pair distribution functions $g(r)$ for Li–Mg alloy are shown in FIG. 1. Overall, the predicted shapes and peak neighbors of pair distribution functions by OF-DFT within NLPPF match the results calculated by KS-DFT. Especially notable are the resulting contributions of the partial distributions [FIG. 1 (b-d)] calculated by OF-DFT within the NLPPF being almost identical to the KS-DFT calculations, which are superior to those obtained by the local pseudopotentials.

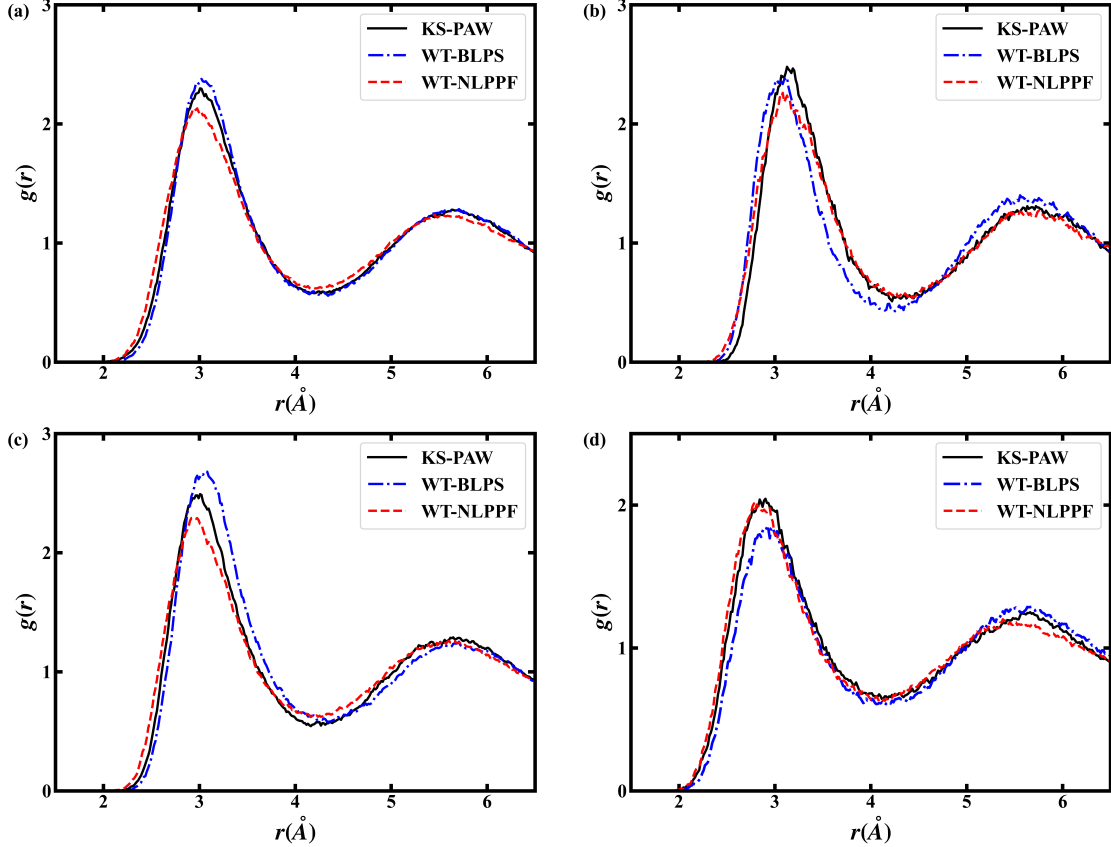


FIG. 1: (a) Total, (b) Mg-Mg partial, (c) Li-Mg partial and (d) Li-Li partial pair distribution functions $g(r)$ of $\text{Li}_{54}\text{Mg}_{54}$ alloy.

To demonstrate the transferability of our scheme, we randomly generated 50 structures of Li systems using CALYPSO[68, 69]. The total energies of these structures were calculated by OF-DFT and KS-DFT. The comparisons of total energy relative to the HCP structure (E_R) are shown in FIG. 2. The orderings of energy are well captured by OF-DFT within NLPPF. The relative energies of different phases are overall well reproduced and in reasonable agreement with the KS-DFT results. The least-square fitting lines of WT-NLPPF are generally closer to the KS-PAW results than those from the local pseudopotentials. For example, the mean error of E_R for Li systems obtained by OF-DFT within the WT-NLPPF is 45 meV/atom, which is lower than that within goLPS (130 meV/atom), BLPS (73 meV/atom), or OEPP (201 meV/atom). Therefore, this framework of OF-DFT with improved transferability is superior to the traditional one.

Previous studies have shown that OF-DFT with local pseudopotentials can be applied to

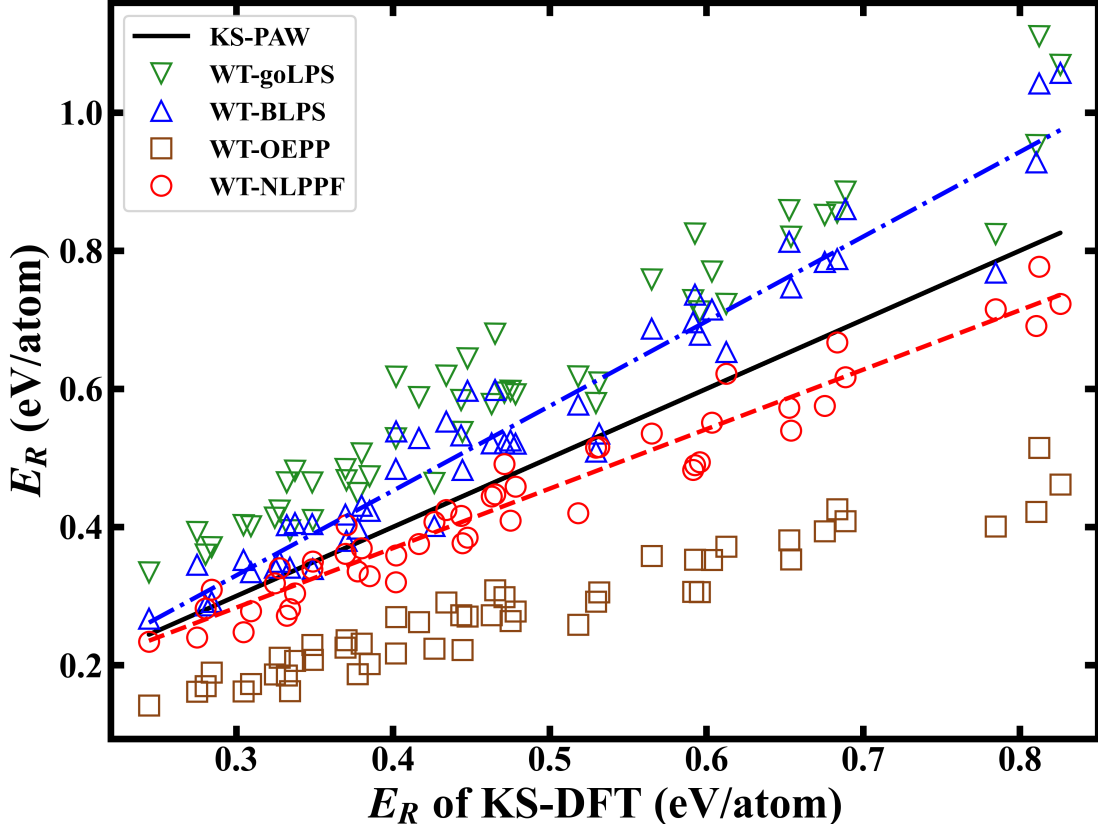


FIG. 2: Relative energies E_R for 50 random structures of Li obtained by OF-DFT using BLPS, OEPP and NLPPF in comparison with KS-DFT using the PAW method. Dot-dash and dashed lines are the least-square fittings of WT-BLPS and WT-NLPPF results, respectively.

most s - and p -block metals. However, OF-DFT simulation using the local pseudopotential OEPP shows unacceptable errors for various crystalline phases of Be (FIG. 3): the curves of energy with respect to volume for HCP and face-centered cubic (FCC) structures show the total energy monotonically decreasing with increasing volume. In contrast, the curves with clear minima predicted by OF-DFT within NLPPF agree well with those produced by KS-DFT. These findings indicate the significant superiority of our proposed framework over the conventional one.

Note that the bulk properties (e.g., equilibrium volume, bulk modulus, and relative energy) calculated by OF-DFT within NLPPF reproduce the results of KS-DFT for Li and Mg almost exactly (TABLE I), considering the maximal deviation of E_R is within 32 meV/atom. However, there are some discrepancies for crystalline phases of Be: in particular, the devi-

TABLE I: B_0 (GPa), E_R (eV/atom) and V_0 ($\text{\AA}^3/\text{atom}$) for bulk Li, Mg, and Be by KS-DFT and OF-DFT.

		Method	HCP	FCC	BCC	SC
Li	B_0	KS-PAW	13.9	13.6	13.9	12.1
		WT-NLPPF	13.5	13.5	13.7	11.0
	V_0	KS-PAW	20.280	20.372	20.396	20.580
		WT-NLPPF	19.483	19.462	19.352	20.844
	E_R	KS-PAW	0.000	0.000	0.001	0.120
		WT-NLPPF	0.000	0.000	0.001	0.152
Mg	B_0	KS-PAW	35.8	35.5	34.8	22.7
		WT-NLPPF	33.0	31.3	31.3	21.2
	V_0	KS-PAW	22.838	23.071	22.826	27.478
		WT-NLPPF	23.194	23.924	23.730	28.274
	E_R	KS-PAW	0.000	0.012	0.029	0.382
		WT-NLPPF	0.000	0.011	0.031	0.372
Be	B_0	KS-PAW	123.3	119.7	124.1	74.5
		WT-NLPPF	91.5	90.5	87.2	63.3
	V_0	KS-PAW	7.910	7.875	7.822	10.274
		WT-NLPPF	7.690	7.942	7.798	10.160
	E_R	KS-PAW	0.000	0.080	0.099	1.004
		WT-NLPPF	0.000	0.058	0.082	0.561

ation of E_R for the simple cubic (SC) phase is larger than 400 meV/atom. To explore the causes of these discrepancies, we estimated the errors of the kinetic energy density of the WT-KEDF with respect to the KS kinetic energy density along the [100] and [111] directions in the SC structures of Li, Mg, and Be (FIG. 4). The kinetic energy density of KS-DFT is clearly reproduced accurately by the WT-KEDF for Li and Mg with slow variations of electron densities. However, it is seriously underestimated for Be, in which the electron distribution rapidly varies in the near-core region. Therefore, we believe that errors in the kinetic energy densities for Be lead to the discrepancy in its bulk properties obtained by

TABLE II: B_0 (GPa), E_R (eV/atom) and V_0 ($\text{\AA}^3/\text{atom}$) for bulk Cd by KS-DFT and OF-DFT.

		Method	HCP	FCC	BCC	SC
Cd	B_0	KS-PAW	40.8	41.0	34.5	29.2
		KS-NLPP	67.4	66.2	66.1	39.8
		WT-OEPP	148.2	138.8	147.1	74.8
		WT-NLPPF	67.0	64.8	65.2	39.8
	V_0	KS-PAW	22.758	22.979	23.512	27.141
		KS-NLPP	15.684	15.851	15.674	18.487
		WT-OEPP	10.379	10.693	10.379	11.964
		WT-NLPPF	15.702	16.027	15.763	18.878
	E_R	KS-PAW	0.000	0.004	0.053	0.121
		KS-NLPP	0.000	0.019	0.036	0.436
		WT-OEPP	0.000	0.138	0.072	0.979
		WT-NLPPF	0.000	0.036	0.056	0.451

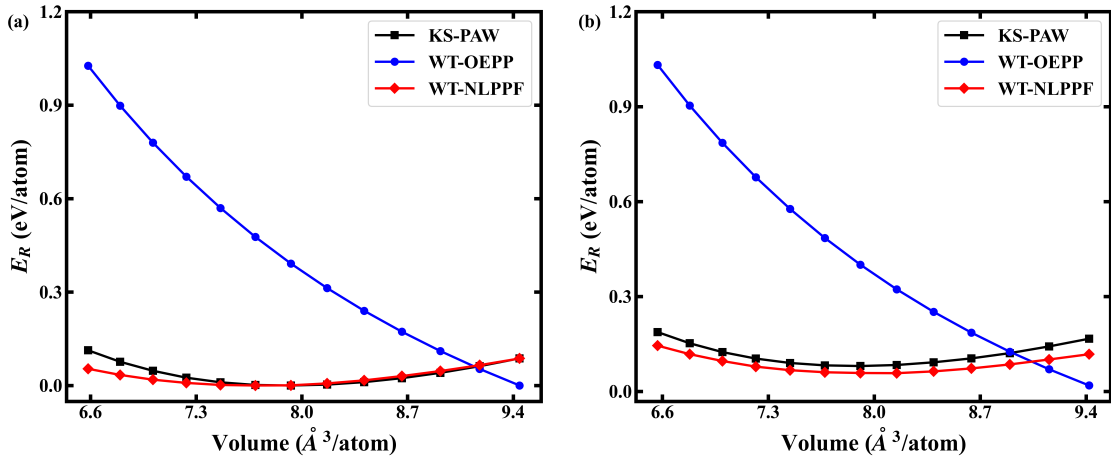


FIG. 3: Relative energy versus volume curves (a) HCP and (b) FCC structures of Be. The total energy shift of WT-OEPP is -33.030 eV/atom.

the framework of OF-DFT within the NLPPF. The findings are fairly consistent with our expectation that the performance of the NLPPF relies strongly on the accuracy of kinetic energy density, as manifested by Eqs. (7) and (8).

To verify our expectation, we calculated bulk properties using OF-DFT and KS-DFT with

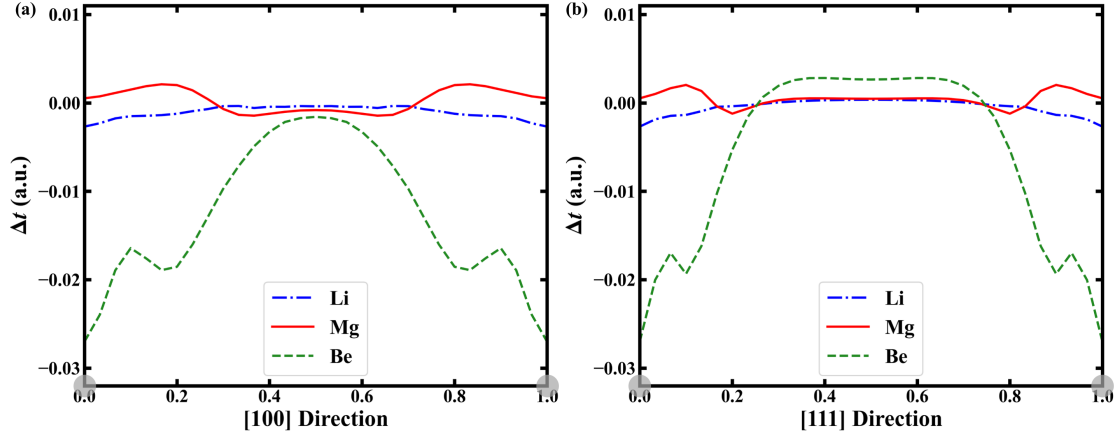


FIG. 4: Kinetic energy density difference along the $\Delta t(\mathbf{r})$ along (a) [100] and (b) [111] directions of Li-/Mg-/Be-SC systems, where $\Delta t(\mathbf{r}) \equiv t_s^{WT}[\rho^{KS}](\mathbf{r}) - t_s^{KS}(\mathbf{r})$.

various pseudopotentials for Cd structures (TABLE II). Note that the NLPP was constructed without the d -channel. The OF-DFT calculations using OEPP gave serious discrepancies compared with KS-NLPP results in all energetic properties, whereas the bulk properties predicted by the OF-DFT within NLPPF framework agree fairly well with the predictions by KS-DFT using the same NLPP. However, there are large discrepancies between OF-DFT using NLPP and KS-DFT using the PAW method for the calculated values of V_0 and B_0 . The strong dependence of the accuracy of OF-DFT on the KEDFs is established; its kinetic energy density also has a strong effect in NLPPF. However, there is no accurate KEDF available for systems with d -channel electrons[54, 55, 70], leading to the failure of OF-DFT using NLPPF when applied to these systems. Therefore, the lack of accurate and general KEDF remains a substantial barrier to the extension of this OF-DFT framework’s application to transition metals or covalent systems.

To assess the computational efficiency of the current scheme, static simulations of Cs body centered cubic supercells containing 128 to 16,000 atoms were performed by OF-DFT within NLPPF. The total wall time of the single point energy calculations is plotted with respect to the number of atoms in FIG. SI of the Supplemental Material. The computational cost of this framework clearly scales linearly with the number of atoms in the simulation cell, in sharp contrast to the cubic scaling of KS-DFT. This shows that the OF-DFT within NLPPF is potentially applicable to the simulation of large-scale systems containing millions of atoms.

In summary, we propose a special scheme of NLPPF that allows the direct use of NLPPs in OF-DFT calculations. The static and dynamic properties of s and p block metals calculated within this scheme agree well with KS-DFT predictions and show significant improvements on the computational accuracy and transferability over conventional OF-DFT with local pseudopotentials. This work defies the conventional wisdom of orbital-dependent NLPPs being incompatible with OF-DFT, leading to the creation of an alternative framework of OF-DFT, which opens up new avenues for further development of the theory.

Q. X., Y. W. and Y. M. acknowledge funding support from the National Natural Science Foundation of China under Grants No. 12047530, 12034009, 91961204, 11774127, 12174142, 11404128, 11822404, and 11974134; the Program for JLU Science and Technology Innovative Research Team. Part of the calculation was performed in the high-performance computing center of Jilin University.

* Electronic address: wyc@calypso.cn

† Electronic address: mym@calypso.cn

- [1] P. Hohenberg and W. Kohn, *Physical Review* **136**, B864 (1964).
- [2] W. Kohn and L. J. Sham, *Physical Review* **140**, A1133 (1965).
- [3] M. Chen, J. Xia, C. Huang, J. M. Dieterich, L. Hung, I. Shin, and E. A. Carter, *Computer Physics Communications* **190**, 228 (2015).
- [4] M. Chen, X.-W. Jiang, H. Zhuang, L.-W. Wang, and E. A. Carter, *Journal of Chemical Theory and Computation* **12**, 2950 (2016).
- [5] X. Shao, Q. Xu, S. Wang, J. Lv, Y. Wang, and Y. Ma, *Computer Physics Communications* **233**, 78 (2018).
- [6] X. Shao, K. Jiang, W. Mi, A. Genova, and M. Pavanello, *Wiley Interdisciplinary Reviews: Computational Molecular Science* **11**, e1482 (2021).
- [7] Y. A. Wang and E. A. Carter, *Orbital-Free Kinetic-Energy Density Functional Theory* (Springer Netherlands, Dordrecht, 2002), pp. 117–184.
- [8] T. A. Wesolowski and Y. A. Wang, *Recent Progress in Orbital-free Density Functional Theory* (World Scientific, 2013).
- [9] L. H. Thomas, *Mathematical Proceedings of the Cambridge Philosophical Society* **23**, 542–548

- (1927).
- [10] E. Fermi, *Rend. Accad. Naz. Lincei* **6**, 5 (1927).
 - [11] E. Fermi, *Zeitschrift für Physik* **48**, 73 (1928).
 - [12] C. v. Weizsäcker, *Zeitschrift für Physik* **96**, 431 (1935).
 - [13] H. Ou-Yang and M. Levy, *Physical Review A* **44**, 54 (1991).
 - [14] J. P. Perdew, *Physics Letters A* **165**, 79 (1992).
 - [15] A. J. Thakkar, *Physical Review A* **46**, 6920 (1992).
 - [16] L. Vitos, B. Johansson, J. Kollar, and H. L. Skriver, *Physical Review A* **61**, 052511 (2000).
 - [17] M. Ernzerhof, *Journal of Molecular Structure: THEOCHEM* **501**, 59 (2000).
 - [18] D. García-Aldea and J. Alvarillos, *The Journal of Chemical Physics* **127**, 144109 (2007).
 - [19] L. A. Constantin and A. Ruzsinszky, *Physical Review B* **79**, 115117 (2009).
 - [20] L. A. Constantin, E. Fabiano, S. Laricchia, and F. Della Sala, *Physical Review Letters* **106**, 186406 (2011).
 - [21] S. Laricchia, E. Fabiano, L. Constantin, and F. Della Sala, *Journal of Chemical Theory and Computation* **7**, 2439 (2011).
 - [22] V. V. Karasiev, D. Chakraborty, O. A. Shukruto, and S. Trickey, *Physical Review B* **88**, 161108 (2013).
 - [23] L. A. Constantin, E. Fabiano, S. Śmiga, and F. Della Sala, *Physical Review B* **95**, 115153 (2017).
 - [24] K. Luo, V. V. Karasiev, and S. Trickey, *Physical Review B* **98**, 041111 (2018).
 - [25] L. A. Constantin, E. Fabiano, and F. Della Sala, *The Journal of Physical Chemistry Letters* **9**, 4385 (2018).
 - [26] K. Luo, V. V. Karasiev, and S. Trickey, *Physical Review B* **101**, 075116 (2020).
 - [27] E. Chacón, J. Alvarillos, and P. Tarazona, *Physical Review B* **32**, 7868 (1985).
 - [28] L.-W. Wang and M. P. Teter, *Physical Review B* **45**, 13196 (1992).
 - [29] E. Smargiassi and P. A. Madden, *Physical Review B* **49**, 5220 (1994).
 - [30] F. Perrot, *Journal of Physics: Condensed Matter* **6**, 431 (1994).
 - [31] Y. A. Wang, N. Govind, and E. A. Carter, *Physical Review B* **58**, 13465 (1998).
 - [32] Y. A. Wang, N. Govind, and E. A. Carter, *Physical Review B* **60**, 16350 (1999).
 - [33] D. Garcia-Aldea and J. Alvarillos, *Physical Review A* **76**, 052504 (2007).
 - [34] C. Huang and E. A. Carter, *Physical Review B* **81**, 045206 (2010).

- [35] L. A. Constantin, E. Fabiano, and F. Della Sala, *Physical Review B* **97**, 205137 (2018).
- [36] W. Mi, A. Genova, and M. Pavanello, *The Journal of Chemical Physics* **148**, 184107 (2018).
- [37] W. Mi and M. Pavanello, *Physical Review B* **100**, 041105 (2019).
- [38] Q. Xu, Y. Wang, and Y. Ma, *Physical Review B* **100**, 205132 (2019).
- [39] Q. Xu, J. Lv, Y. Wang, and Y. Ma, *Physical Review B* **101**, 045110 (2020).
- [40] B. Zhou, Y. A. Wang, and E. A. Carter, *Physical Review B* **69**, 125109 (2004).
- [41] C. Huang and E. A. Carter, *Physical Chemistry Chemical Physics* **10**, 7109 (2008).
- [42] B. G. del Rio and L. E. Gonzalez, *Journal of Physics: Condensed Matter* **26**, 465102 (2014).
- [43] W. Mi, S. Zhang, Y. Wang, Y. Ma, and M. Miao, *The Journal of Chemical Physics* **144**, 134108 (2016).
- [44] B. G. Del Rio, J. M. Dieterich, and E. A. Carter, *Journal of Chemical Theory and Computation* **13**, 3684 (2017).
- [45] X. Shao, W. Mi, and M. Pavanello, *Phys. Rev. B* **104**, 045118 (2021).
- [46] D. Hamann, M. Schlüter, and C. Chiang, *Physical Review Letters* **43**, 1494 (1979).
- [47] M. Fuchs and M. Scheffler, *Computer Physics Communications* **119**, 67 (1999).
- [48] R. M. Martin, *Electronic Structure: Basic Theory and Practical Methods* (Cambridge University Press, 2004).
- [49] J. Lehtomäki, I. Makkonen, M. A. Caro, A. Harju, and O. Lopez-Acevedo, *The Journal of Chemical Physics* **141**, 234102 (2014).
- [50] V. Zavodinsky and O. A. Gorkusha, *Nanosystems: Physics, Chemistry, Mathematics* **10**, 402 (2019).
- [51] D. Vanderbilt, *Physical review B* **41**, 7892 (1990).
- [52] W. C. Witt, B. G. Del Rio, J. M. Dieterich, and E. A. Carter, *Journal of Materials Research* **33**, 777 (2018).
- [53] W. C. Witt, B. W. Shires, C. W. Tan, W. J. Jankowski, and C. J. Pickard, *The Journal of Physical Chemistry A* **125**, 1650 (2021).
- [54] Y. Ke, F. Libisch, J. Xia, L.-W. Wang, and E. A. Carter, *Physical Review Letters* **111**, 066402 (2013).
- [55] Y. Ke, F. Libisch, J. Xia, and E. A. Carter, *Physical Review B* **89**, 155112 (2014).
- [56] D. Chakraborty, R. Cuevas-Saavedra, and P. W. Ayers, *Theoretical Chemistry Accounts* **136**, 1 (2017).

- [57] D. Chakraborty, R. Cuevas-Saavedra, and P. W. Ayers, *Kinetic Energy Density Functionals from Models for the One-Electron Reduced Density Matrix* (Springer International Publishing, Cham, 2018), pp. 199–208.
- [58] L. Kleinman and D. Bylander, *Physical Review Letters* **48**, 1425 (1982).
- [59] N. Troullier and J. L. Martins, *Physical Review B* **43**, 1993 (1991).
- [60] C. Lee and R. G. Parr, *Physical Review A* **35**, 2377 (1987).
- [61] M. Berkowitz, *Chemical Physics Letters* **129**, 486 (1986).
- [62] R. G. Parr and W. Yang, *Density-Functional Theory of Atoms and Molecules* (New York: Oxford University Press, 1989).
- [63] S. K. Ghosh, M. Berkowitz, and R. G. Parr, *Proceedings of the National Academy of Sciences* **81**, 8028 (1984).
- [64] See Supplemental Material for the detailed KED of WT, the computational details, and the numerical results of the the bulk properties for Li/Mg/K/Cs/Zn systems by OF-DFT and KS-DFT. (2021).
- [65] W. Mi, X. Shao, C. Su, Y. Zhou, S. Zhang, Q. Li, H. Wang, L. Zhang, M. Miao, Y. Wang, et al., *Computer Physics Communications* **200**, 87 (2016).
- [66] F. Murnaghan, *J. Franklin Inst.* **197**, 98 (1924).
- [67] P. E. Blöchl, *Physical Review B* **50**, 17953 (1994).
- [68] Y. Wang, J. Lv, L. Zhu, and Y. Ma, *Physical Review B* **82**, 094116 (2010).
- [69] Y. Wang, J. Lv, L. Zhu, and Y. Ma, *Computer Physics Communications* **183**, 2063 (2012).
- [70] C. Huang and E. A. Carter, *Physical Review B* **85**, 045126 (2012).